NBSIR 78-1558

Development of Hydrogen and Hydroxyl Contamination in Thin Silicon Dioxide Thermal Films

Santos Mayo

Electron Devices Division
Center for Electronics and
   Electrical Engineering
National Engineering Laboratory

and

William H. Evans

Chemical Thermodynamics Division
Center for Thermodynamics and
   Molecular Science
National Measurement Laboratory
U.S. Department of Commerce
National Bureau of Standards
Washington, DC 20234

March 1979

Final

NBSIR 78-1558

DEVELOPMENT OF HYDROGEN AND HYDROXYL CONTAMINATION IN THIN SILICON DIOXIDE THERMAL FILMS

Santos Mayo

Electron Devices Division
Center for Electronics and
Electrical Engineering
National Engineering Laboratory

and

William H. Evans

Chemical Thermodynamics Division
Center for Thermodynamics and
Molecular Science
National Measurement Laboratory
U.S.Department of Commerce
National Bureau of Standards
Washington, DC 20234

March 1979

Final

TABLE OF CONTENTS

iii

LIST OF TABLES

Development of Hydrogen and Hydroxyl Contamination
in Thin Silicon Dioxide Thermal Films

Santos Mayo
Electron Devices Division
Center for Electronics and Electrical Engineering
National Engineering Laboratory

and

William H. Evans
Chemical Thermodynamics Division
Center for Thermodynamics and Molecular Science
National Measurement Laboratory

National Bureau of Standards
Washington, DC 20234

ABSTRACT

Hydrogen and hydroxyl incorporation into thin silicon dioxide
films thermally grown on silicon in dry oxygen atmospheres
contained in resistance-heated fused silica or polycrystalline
silicon tubes is analyzed. The mechanisms leading to incor-
poration of these impurities in the film are discussed in
terms of trace water and hydrocarbon contamination in the oxy-
gen used, room ambient humidity permeation through the fused
silica tube, the silicon wafer preparation prior to oxidation,
and other environment factors. The most significant reactions
occurring in the water-silica-silicon system during wafer oxi-
dation at temperatures in the range from 800°C to 1200°C are
discussed. It is shown that, during the oxidation period re-
quired to grow a 100-nm thick silicon dioxide film on a <100>
silicon wafer in nominally dry oxygen containing water con-
tamination in the ppm range, the introduction of hydrogen and

1

hydroxyl contamination into the oxide film can be explained
in terms of the water-silica interaction. The use of poly-
crystalline silicon oxidation tubes is discussed with refer-
ence to the inherent water gettering action of silicon at
oxidation temperatures.

Key Words: Dry oxidation of silicon; hydrogen contamination;
hydroxyl contamination; semiconductor device fabrication;
silicon; silicon dioxide; thermal oxidation of silicon.

INTRODUCTION

Ionic contamination in thermally grown thin silicon dioxide films is
known to cause instability in microelectronic devices [1]. In addition
to alkali ions, protons are generally identified as a mobile ionic spe-
cies responsible for such instability in silicon dioxide films. While
the contamination mechanism leading to alkali and heavy ion inclusion
in these films has been discussed [2], mechanisms for incorporation of
hydrogen and hydroxyl impurities in thermally grown silicon dioxide
films have not been extensively analyzed. Infrared studies have shown
significant amounts of these impurities in silicon dioxide films [3],
when either fused silica or polysilicon tubes are used to contain the
the oxidation atmosphere [4]. These results suggest a strong correla-
tion between water contamination in the oxidation atmosphere and hydro-
gen and hydroxyl contamination in the films.

At oxidation temperatures, trace amounts of hydrogen or hydrogen-
containing species in the atmosphere or included on the wafer causes
strong interactions with the silicon-silica system resulting in the in-

2

corporation of hydrogen-bearing species into the growing silica film. This type of impurity on the wafer surface has been shown to have a marked influence on the oxidation rate of silicon [5]. If a thin hydrolyzed oxide layer is present on the wafer surface prior to thermal oxidation, the oxidation rate is reduced with respect to nonhydrolyzed silicon, suggesting a significant alteration has been produced at the silicon-silica interface. A number of species containing hydrogen and hydroxyl-bonded silicon have been reported in this interface layer [6].

At room temperature, oxygen, water, and hydrocarbons from the room ambient adsorb on clean silicon forming a thin film containing hydrogen-bearing compounds on the wafer surface prior to the thermal oxidation [7]. The oxygen-silicon bond in this film is stable enough (heat of adsorption 210 kcal/mole) to remain on the wafer surface and, consequently, influence the initial kinetics during the thermal oxidation of silicon [8]. The presence of complex structures such as SiO_3 in these absorbed films has been reported even for cases in which less than a monolayer of oxygen is adsorbed on the silicon surface [9]. The thickness of both hydrogen and water adsorbed layers was found to be dependent on the wafer polishing procedure [10]. The wafer preparation procedure requires strict material and environmental control to secure stable and reproducible thermal oxidation results.

In this paper, an estimate of the hydrogen and the hydroxyl content in thermally grown thin silicon dioxide films prepared in oxidation atmospheres enclosed in resistance-heated fused silica or polycrystalline silicon tubes is presented. The results are compared with

3

available hydrogen and hydroxyl density data measured by infrared
internal reflection spectroscopy (IRS) [3,4].

WATER CONTAMINATION IN OXIDATION ATMOSPHERES

The origin of water contamination in dry oxygen atmospheres used to
grow silicon dioxide films on silicon is related to impurities in
the oxygen and permeation of water from the room ambient through the
furnace tube [11-13]. Electronic grade oxygen generally contains about
5 ppm water and 20 ppm hydrocarbons [11]. At oxidation temperatures,
the hydrocarbons decompose in the oxidation atmosphere to form car-
bon dioxide and water, resulting in about 25 ppm water contamination.
To reduce this contamination level, oxygen needs to be purified be-
fore being used in the oxidation chamber. Hydrocarbons are removed
by cracking at high temperatures, and water is removed by subsequent
condensation at an appropriate low temperature. Oxygen treated in
this way contains about 1 ppm water [12,14].

At high temperatures, water dissociates to form hydroxyl and hydrogen.
However, the amount of these dissociation products is relatively small,
and consequently water remains the most important impurity to interact
with the silicon-silica system. For example, at 1300 K the equilibrium
of water and its dissociation products in oxygen [2] corresponds to
partial pressure ratios of:

$$P(OH)/P(H_2O) = 5 \times 10^{-2},$$
$$P(H)/P(H_2O) = 3 \times 10^{-7}, \text{ and}$$
$$P(H_2O) = 3 \times 10^{-8}.$$

4

Table 1 shows the equilibrium constants for water-induced reactions oc-
curring in the thermal oxidation of silicon contained in a nominally
dry atmosphere at 1300 K. Table 2 shows the thermodynamic data used for
these calculations; values for the standard enthalpy of formation and
the Gibbs free energy function in the standard state at 1300 K are from
JANAF tables [15] or from high temperature water-silica reaction data
[16].

Some reactions listed in table 1 exhibit large equilibrium constants
indicative of the tendency of the reaction to occur. Due to the lack
of reaction kinetic data, the exact amount of water incorporated into
the oxide film during the oxidation period cannot be determined. How-
ever, qualitative considerations can be used to estimate the expected
water contamination in such films. For example, in 1 atm oxygen con-
taining 1 ppm water at 1000°C, the water number density is $5.7 \times
10^{12}$ cm^{-3} and the average water molecular velocity is 1.2×10^5 $cm \cdot s^{-1}$
[17]. It takes approximately 175 min to grow a 100-nm thick oxide film
on <100> silicon in this atmosphere. During this oxidation period,
water molecules impinge on the wafer reacting with the growing film
and some of these molecules become incorporated into the film. The
water fluence on the wafer is [17]:

$$F = 2.67 \times 10^{25} \; P \; t/(W \; T)^{1/2} = 1.85 \times 10^{21} \; cm^{-2}$$

where P is the water partial pressure in the oxidation ambient (in
atmospheres), t is the wafer oxidation period (in seconds), W = 18 g is
the molecular weight of water; and T = 1273 K, is the absolute tem-
perature. The water fraction (η) incorporated into the film can be

5

estimated from data on water oxidation of silicon in inert atmospheres; η is determined by the silica film thickness and the water fluence on the wafer F:

$$\eta = x\rho N/WF$$

where x is the silica film thickness grown by water oxidation of silicon (in centimeters), $\rho = 2.3$ $g \cdot cm^{-3}$ is the film density; N is Avogadro's number; and W = 60 g, is the molecular weight of silica. From available data on the oxidation of silicon at 1000° C in inert atmospheres containing trace water contamination, η is estimated in the 10^{-9} range* [18,19]. In 100-nm thick silica films grown on <100> silicon at 1000°C in 1 atm oxygen containing 1 ppm water contamination, the expected water number density is in the 10^{17} cm^{-3} range. This figure is close to the solubility of water in fused silica at 1000°C exposed to an inert atmosphere with water partial pressure $P(H_2O) =$ 10^{-6} atm [20,21]. Consequently, silica films grown on silicon in a conventional dry oxidation facility are expected to exhibit water contamination up to the solubility equilibrium determined by the temperature and the water partial pressure in the oxidation ambient. Table 3

---

*T. Nakayama and F. C. Collins [19] reported on the oxidation of silicon in 1 atm argon with water partial pressure in the range 10^{-3} atm $\leq P(H_2O) \leq 10^{-1}$ atm. These data agree with results obtained in 1 atm nitrogen containing trace water contamination [18]. However, their data on nominally dry argon [$P(H_2O) = 0$ atm] do not agree with other results [18]. The authors indicate that the oxide growth rate in nominally dry argon at 1000°C can only be explained if the water impurity in argon is assumed to be 460 ppm. This rather large contamination may arise from oil vapor backstreaming from an oil bubbler used to close the exit port of the furnace tube to prevent entrance of atmospheric moisture. At oxidation temperatures, cracking of oil in oxygen generates enough water to explain the data obtained for oxidation in nominally dry argon.

summarizes calculations made for films grown in 1 atm oxygen containing 1 ppm water or 125 ppm water at temperatures in the range 780°C to 1200°C.

These results are in agreement with diffusion data. If an ideally dry silica film is exposed to a water-contaminated inert atmosphere at oxidation temperatures, the water diffusion through the film is high enough to account for water saturation of the film during an interval of time equivalent to the oxidation period. For example, a 100-nm thick pure silicon dioxide film exposed to 1 atm nitrogen containing 1 ppm water at 1000°C allows the diffusion of 4.1×10^8 $cm^{-2} \cdot s^{-1}$ water molecules (the diffusion coefficient of water in silica at 1000°C is 7.2×10^{-10} $cm^2 \cdot s^{-1}$ [20,21]). Assuming this film is exposed for 175 min (equivalent to the time necessary to grow at 1000°C a 100-nm thick oxide film on silicon in oxygen at atmospheric pressure containing 1 ppm water), the water diffused through the film is 4.3×10^{12} cm^{-2}, and the resulting water number density in the film is 4.3×10^{17} cm^{-3}. This figure agrees in order of magnitude with the estimated water number density in the film due to water reactivity with the silica-silicon system during the oxidation period. Both the water kinetic consideration in the oxidation atmosphere and the water diffusion into the film provide coincident results.

In addition to water diffusion, hydrogen diffusion through the film plays an important role. Although the hydrogen content in the oxidation atmosphere is small, its diffusion coefficient in silica and

silicon is large.* It has been postulated that the formation of triva-
lent silicon compounds at the silicon-silica interface are generally
associated with structurally defective sites in the silicon and silica
lattices where interstitial hydrogen plays a key role in reactions with
trivalent silicon exhibiting nonsaturated dangling bonds [23]. The
resulting silicon-hydrogen structures are thought to affect the elec-
trical properties and the radiation response of silicon microelectronic
devices, and therefore the presence of hydrogen might become a factor
of major technological significance.

INFLUENCE OF THE FURNACE TUBE ON THERMALLY GROWN SILICON DIOXIDE FILMS
It has been shown that alkali and other impurities included in fused
silica tubes can evaporate into the oxidation atmosphere and contami-
nate the growing oxide films [2]. Similarly, hydroxyl may evaporate
from fused silica tubes containing water as an impurity. There are
two types of fused silica available as tube material: natural and
synthetic. The former is made by electrical fusion of quartz-crystal
powder resulting in a product containing about 10 ppm hydroxyl and 100
to 200 ppm metallic impurity. Synthetic fused silica is made by flame
fusion of highly purified chemicals and results in a product contain-
ing about 3000 ppm hydroxyl and less than 2 ppm metallic impurity [24].
Furnace tubes used in oxidation facilities are generally made out of
natural fused silica with low hydroxyl content. However, since the

---

*At 1000°C the hydrogen-to-water partial-pressure ratio in 1 atm oxy-
gen containing 1 ppm water is 3×10^{-7}. The diffusion coefficient of
hydrogen in silicon is 10^{-4} cm$^2 \cdot$s^{-1} and in silica is 10^{-5} cm$^2 \cdot$s [22].

tube is constantly exposed to room humidity, its hydroxyl content increases up to the solubility limit.

It has been suggested [12,13] that water from the room ambient permeates through the fused silica furnace tube adding impurity to the oxidation atmosphere. Assuming that the oxidation facility is in a room with an ambient temperature of 25°C and a relative humidity of 30 percent, the resulting water partial pressure in this room is 9.4×10^{-3} atm [25]. The corresponding water number density in the proximity of the oxidation tube at 1000°C is 5.4×10^{16} cm^{-3}. When water comes in contact with the tube wall, it dissociates forming silanol which is incorporated into the fused silica:

$$H_2O(g) + (\equiv Si - 0 - Si \equiv) \ (c) \overset{\leftarrow}{\to} 2(\equiv Si - OH) \ (c).$$
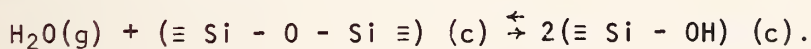
At oxidation temperatures, this process reaches equilibrium in a few days [20] resulting in a constant water concentration in the bulk determined by the hydroxyl solubility in fused silica. This is 7×10^{18} cm^{-3} or about 300 ppm for fused silica exposed to a partial pressure of water $P(H_2O) = 9.4 \times 10^{-3}$ at 1000°C [21]. The evaporation of hydroxyl groups into the oxidation atmosphere can be calculated assuming the wall as a constant concentration source. At constant temperature, hydroxyl in silica diffuses out at a smaller rate than it diffuses in [20,21], and so the tube reaches equilibrium hydroxyl concentration in a relatively short time.

Table 4 shows the available data and the resulting hydroxyl partial pressure in the oxidation atmosphere due to water permeation through the tube wall. For example, at 1000°C the water flux entering into

9

this atmosphere is 2×10^{10} $cm^{-2} \cdot s^{-1}$. These molecules are emitted from the tube wall. For example, at 1000°C the water flux entering into this atmosphere is 2×10^{10} $cm^{-2} \cdot s^{-1}$. These molecules are emitted from the tube wall with average velocity $v = (8\ kT/m\pi)^{\frac{1}{2}} = 1.2 \times 10^{5}$ $cm \cdot s^{-1}$ and diffuse in the oxygen with a diffusion coefficient $D(OH\text{-}O_2)$ calculated according to [17]:

$$D(OH\text{-}O_2) = (v^2(OH) + v^2(O_2))^{\frac{1}{2}}/3\pi n\delta^2 \approx 1.7\ cm^2 \cdot s^{-1},$$

where $n = 5.7 \times 10^{18}$ cm^{-3} is the oxygen number density in the oxidation ambient at 1 atm and 1000°C, and $\delta = (\delta(OH) + \delta(O_2))/2 = 4.1 \times 10^{-8}$ cm is the $OH\text{-}O_2$ molecular diameter.* The net hydroxyl molecular displacement per unit time t (measured in seconds) in any arbitrary direction in the oxidation atmosphere can be expressed as [17]: $z_r = (2tD(OH\text{-}O_2))^{\frac{1}{2}} = 1.8$ cm. The hydroxyl number density in the oxidation atmosphere is estimated from the net displacement in a direction perpendicular to the wall. This displacement generates a 1.8 cm^3 volume per unit wall area and unit time. This volume contains a number of hydroxyl molecules given by the net balance between the incoming and the outgoing fluxes. This number is 2×10^{10} $cm^{-2} \cdot s^{-1}/1.8$ $cm \cdot s^{-1} = 1.1 \times 10^{10}$ cm^{-3}, and the corresponding partial pressure in the oxidation atmosphere is $P(OH) = 1.9 \times 10^{-9}$ atm. This pressure is 26 times smaller than the hydroxyl equilibrium partial pressure generated from dissociation of 1 ppm water in oxygen.

---

*Another approximate expression can be used to evaluate the interdiffusion coefficient of hydroxyl in oxygen: $D = 2(k^3T^3/\pi^3m)^{\frac{1}{2}}/d\pi^2P$; here, $P = 1$ atm is the oxygen pressure [26]. At 1000°C, $D = 0.76$ $cm^2 \cdot s^{-1}$; the difference between this and the D-value calculated above is not significant for the purpose of this discussion.

Consequently, the use of natural fused silica tubes in oxidation
furnaces does not necessarily ensure low hydroxyl content in the oxida-
tion atmosphere.   In addition, natural fused silica has about 100 times
more metallic impurity than synthetic fused silica, so the criteria
used to select the furnace oxidation tube need to be reexamined.[*]

The use of polycrystalline silicon tubes in oxidation furnaces instead
of fused silica presents interesting aspects.   Water permeation through
the tube wall is greatly reduced since water reacts with silicon to
form a silica "skin" on the tube wall:

$$Si(c) + H_2O(g) \rightarrow SiO_2(c) + 2 H_2(g).$$
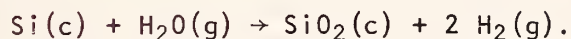
This is the most probable reaction occurring in the oxidation of sili-
con by water and is known to occur rapidly at high temperature.   Thus,
water from the room ambient is preferentially trapped on the tube wall.
In addition to this, the use of polycrystalline silicon tubes allows
the use of higher temperatures in the oxidation of silicon wafers,
thus reducing the oxidation period and, consequently, the water in-
corporation into the growing oxide film.   For example, it takes 59
min to grow a 100-nm thick silicon dioxide film on <100> silicon
at 1100°C in 1 atm oxygen containing 1 ppm water [18]; the total num-
ber of water-silica collisions during this period is 6×10^{20} cm^{-2}.
This is three times less than expected at 1000°C.

_____

[*]Although thermal oxidation of silicon by rf-heating is not generally
used in production-oriented facilities, it is worth noting that it
provides a way of minimizing the tube influence on the oxidation
atmosphere, since the tube remains much cooler than the wafer [27].

11

When a new polycrystalline silicon tube is used, the tube surface area exposed to the oxidation atmosphere is much larger than its geometrical size due to the nature of the polycrystalline surface. This surface reacts quickly with residual water to form silica. This is especially efficient at higher temperature. The wall behaves like a getter removing water from the oxidation atmosphere. Consequently, silica films grown on silicon wafers at high temperatures in dry oxidation atmospheres contained in polycrystalline silicon tubes are expected to show less water contamination than films grown in fused silica tubes under similar conditions. This is an interpretation consistent with a general trend shown by infrared spectroscopic measurements of hydroxyl and hydrogen in thin silicon dioxide films thermally grown in dry atmospheres contained in fused silica or polycrystalline silicon tubes at 1000°C [4]. Naturally, as the silicon tube develops a silica "skin," its gettering action is reduced. Periodic *in situ* cleaning is needed to eliminate the film and regenerate the fresh polycrystalline surface.

MEASUREMENT OF HYDROGEN AND HYDROXYL CONTAMINATION IN THIN SILICON DIOXIDE FILMS

The use of infrared internal reflection spectroscopy (IRS) has been reported for direct measurements of hydrogen and hydroxyl impurity included in thin silicon dioxide films thermally grown in dry oxidation atmospheres contained in both fused silica [3] and polycrystalline silicon tubes [4]. The technique [28] requires the use of trapezoidal silicon prisms on which oxide films are grown. The specimen is exposed to infrared light incident on the prism at an angle

12

appropriate for multiple total internal reflection. Since the index of refraction in the film is lower than the index of refraction in the prism, at each reflection site where total internal reflection occurs at the silicon-silicon dioxide interface, a certain amount of light propogates into the film as an evanescent wave. This evanescent wave travels an unknown distance along the film and then is reflected back into the prism. The only relevant information obtained is due to light absorbed in the film at each reflection. The higher the number of internal reflections in the film, the higher the absorption effect. Depending on the film thickness, the evanescent wave may reach the outer film interface (silicon dioxide/air) where again a similar situation is observed [29].

IRS results were reported on hydrogen and hydroxyl compounds in thin silicon dioxide films thermally grown in dry oxidation atmospheres at 1000°C contained in fused silica or polycrystalline silicon tubes. The oxide films were subsequently annealed in nitrogen for 30 min before being removed from the furnace tube. The results show an order of magnitude reduction in both hydrogen and hydroxyl compounds in silcon dioxide when the polycrystalline silicon tubes are used in the oxidation furnace. The reported values for hydroxyl and hydrogen densities are, respectively 1.7×10^{21} cm^{-3} and 1.7×10^{22} cm^{-3} in films grown in fused silica tubes and 2.9×10^{20} cm^{-3} and 1.8×10^{21} cm^{-3} in films grown in a polycrystalline silicon tube. [4].

Quantitive measurements with this technique require complete knowledge of parameters such as the absorption coefficient of the film, the

13

optical path in the film, and the probe intensity. All of these are difficult to measure. For example, as pointed out elsewhere [3], the evaluation of IRS signals in terms of impurity number density in the film requires knowledge of the effective charge associated with each molecule where the absorbing group is attached. For hydrogen and hydroxyl compounds in silicon dioxide, this information is not complete. The experimental error of IRS measurements is ±50 percent and the sensitivity is 5×10^{18} cm^{-3} for SiOH and 3×10^{19} cm^{-3} for SiH groups [3]. Results obtained on 1-μm thick silicon dioxide films thermally grown at 1100°C in 1 atm oxygen containing 60 ppm water show no SiOH signal ($<5 \times 10^{18}$ cm^{-3}) and 7×10^{19} cm^{-3} SiH [3].

These figures agree in order of magnitude with expected film contamination resulting from interaction with residual water in the oxidation atmosphere. The water fluence on this film during the oxidation period is of the 10^{24} cm^{-2} order of magnitude. Assuming $\eta = 10^{-9}$ for the water-to-silica-silicon interaction, the expected water number density in this film is in the 10^{19} cm^{-3} range.

Although these kinetic considerations are in agreement with IRS results on thin silica films, independent measurements aimed at characterizing hydrogen and hydroxyl impurities in these films are needed. Laser calorimetry may offer this possibility. The technique has already been successfully employed for measurements of very small absorptivities in thin films used for optical applications [30,31]. An extension of this work for thin silicon dioxide films on silicon may provide valuable results to complement available IRS data. Another interesting

technique for hydrogen detection in thin silicon dioxide films using nuclear resonance reactions has been reported [32]. This technique is sensitive to elemental composition and does not provide information on the compound structure into which hydrogen is incorporated.

CONCLUSIONS

Hydrogen and hydroxyl contamination in thin oxide films thermally grown on silicon in nominally dry oxidation atmospheres is primarily due to trace water and hydrocarbons included in the oxygen. The preparation procedure prior to thermal oxidation of silicon may contribute additional oxide contamination included as a very thin layer formed on the silicon wafer. This layer contains hydrogen-bonded and hydroxyl-bonded species that influence the silicon oxidation rate. A minor hydroxyl contamination may result in the oxidation atmosphere due to evaporation from fused silica furnace tubes. A water content below 1 ppm in the oxidation atmosphere can only be achieved when special care is taken in controlling factors such as the prepurification of oxygen, the wafer preparation procedure prior to oxidation, and the furnace tube quality. Complete water contamination removal from the oxidation atmosphere is difficult and expensive; the use of polycrystalline silicon tubes to contain such atmospheres at high oxidation temperatures is preferred to getter residual hydrogen and hydroxyl.

In summary, to minimize hydrogen and hydroxyl impurities in thermally grown thin silicon dioxide films control must be exercised on the water contamination that may arise from (a) oxygen, (b) residual wafer impurity due to the processing, (c) room ambient humidity, and (d) the

15

furnace oxidation tube. The measurement technique used to detect hydrogen and hydroxyl content in these films needs to be carefully examined.

ACKNOWLEDGMENTS

REFERENCES

1. Schlegel, E. S., A Bibliography of Metal-Insulator-Semiconductor Studies, *IEEE Trans. Electron Devices* ED-14, 729-749 (1967), and Additional Bibliography of Metal-Insulator-Semiconductor Studies, *ibid.* ED-15, 951-954 (1968). This is a bibliographic review summarizing early work in this field.

2. Mayo, S., and Evans, W. H., Development of Sodium Contamination in Semiconductor Oxidation Atmospheres at 1000°C, *J. Electrochem. Soc.* 124, 780-785 (1977), and Thermodynamic Considerations in the Use of Polycrystalline Oxidation Tubes for Clean SiO_2 Film Preparation, *J. Electrochem. Soc.* 125, 106-110 (1978).

3. Beckman, K. H., and Harrick, N. J., Hydrides and Hydroxyls in Thin Silicon Dioxide Films, *J. Electrochem. Soc.* 118, 614-619 (1971).

4. Hughes, H., and Pankey, T., private communication, quoted in Revesz, A. G., On SiOH and SiH Groups in SiO_2 Films on Silicon, *J. Electrochem. Soc.* 124, 1811-1813 (1977).

5. Schwettmann, F. N., Chiang, K. L., and Brown, W. A., Variation of Silicon Dioxide Growth Rate with Pre-Oxidation Clean, *Electrochem. Soc. Ext. Abs. 78-1*, Abstract 276, Seattle, Washington, May 21-26, 1978.

6. Grunthaner, F. J., and Maserjian, J., Experimental Observations of the Chemistry of the SiO_2/Si Interface, *IEEE Trans. Nucl. Sci.* NS-24, 2108-2112 (1977).

7. Fujiwara, K., Ogata, H., and Mishijima, M., Adsorption of H_2S, H_2O, and O_2 on Si (111) Surfaces, *Solid State Commun.* 21, 895-897 (1977), and Fujiwara, K., and Mishijima, M., Adsorption of Water Vapor on Si (111) Surfaces, *Phys. Lett.* 55, 211-212 (1975).

8. Bootsa, G. A., Calorimetric Study of the Adsorption of Oxygen and Gases H_xA on Germanium and Silicon, *Surf. Sci.* 15, 340-344 (1969).

9. Mayer, F., and Vrakking, J. J., The Adsorption of Oxygen on a Clean Silicon Surface, *Surf. Sci.* 38, 275-281 (1973).

10. Palik, E. D., Gibson, J. W., Holm, R. T., Hass, M., Braunstein, M., and Garcia, B. Infrared Characterization of Surfaces and Coatings by Internal-Reflection Spectroscopy, *Appl. Opt.* 17, 1776-1785 (1978).

11. Irene, E. A., The Effects of Trace Amounts of Water on the Thermal Oxidation of Silicon in Oxygen, *J. Electrochem. Soc.* 121, 1613-1616 (1974), and Irene, E. A., and van der Meulen, Y. J., Silicon

Oxidation Studies: Analysis of SiO_2 Film Growth Data, *J. Electro-chem. Soc.* <u>124</u>, 1380-1384 (1977).

12. Burkhardt, P. J., and Gregor, L. V., Kinetics of the Thermal Oxi-dation of Silicon in Dry Oxygen, *Trans. Metall. Soc. AIME* <u>236</u>, 299-305 (1966).

13. Revesz, A. G., Non-crystalline Silicon Dioxide Films on Silicon: A Review, *J. Non-Cryst. Solids* <u>11</u>, 309-330 (1973).

14. Ormond, D. W. Irene, E. A., Balgin, J. E., and Crowder, B. L., Expansion of Thermally Grown SiO_2 Thin Films Upon Irradiation With Energetic Ions, *Ion Implantation in Semiconductors 1976*, F. Chernow, J. A., Borders, and D. C. Brice, Eds, pp. 305-317 (Plenum Press, New York, 1977).

15. JANAF Thermochemical Tables, D. R. Stull and H. Prophet, Eds, 2nd ed., NSRDS-NBS 37 (1971).

16. Krikorian, O. H., Thermodynamics of the Silica-Steam System, *Proc. Symp. Engineering with Nuclear Explosives*, Conf. 700101, Vol. 1, pp. 481-492, Las Vegas, Nevada (1970).

17. Dushman, S., *Scientific Foundations of Vacuum Technique*, 2nd ed., Chapters 1 and 2 (J. Wiley and Sons, Inc., New York, 1962).

18. Irene, E. A., and Ghez, R., Silicon Oxidation Studies: The Role of H_2O, *Semiconductor Silicon 1977*, H. R. Huff and E. Sirtl, Eds, pp. 313-323 (The Electrochemical Society, Inc., Princeton, New Jersey, 1977); also published in *J. Electrochem. Soc.* <u>124</u>, 1757-1761 (1977).

19. Nakayam, T., and Collins, F. C., Kinetics of Thermal Growth of Silicon Dioxide Films in Water Vapor-Oxygen-Argon Mixtures, *J. Electrochem. Soc.* <u>113</u>, 706-713 (1966).

20. Hetherington, A. G., and Jack, K. H., Water in Vitreous Silica. Part 1: Influence of "Water" Content on the Properties of Vitreous Silica, *Phys. Chem. Glasses* <u>3</u> (4), 129-133 (1962), and Bell, T., Hetherington, A. G., and Jack, K. H., Water in Vitreous Silica. Part 11: Some Aspects of Hydrogen-Water-Silica Equi-libria, *Phys. Chem. Glasses* <u>3</u> (5), 141-146 (1962).

21. Moulson, A. J., and Roberts, J. P., Water in Silica Glass, *Trans. Faraday Soc.* <u>57</u>, 1208-1216 (1961), and Water in Silica Glass, *Trans. Br. Ceram. Soc.* <u>59</u>, 388-399 (1960).

22. Wolf, H. F., *Silicon Semiconductor Data*, pp. 526-527 (Pergamon Press, Oxford, 1969).

23. Svensson, C. M., The Defect Structure of the $Si-SiO_2$ Interface, A Model Based on Trivalent Silicon and Its Hydrogen "Compounds,"

The Physics of SiO₂ and Its Interfaces, S. T. Pantelides, Ed, pp. 328-332 (Pergamon Press, New York, 1978).

24. Lee, R. W., Diffusion of Hydrogen in Natural and Synthetic Fused Quartz, *J. Chem. Phys.* <u>38</u>, 448-455 (1963).

25. Smithsonian Meteorological Tables, 6th ed., Table 94, pp. 350-353 (Smithsonian Institution, Washington, DC, 1951).

26. Roth, A., *Vacuum Technology*, p. 46 (North Holland Publishing Company, New York, 1976).

27. Revesz, A. G., and Evans, R. J., Kinetics and Mechanism of Thermal Oxidation of Silicon with Special Emphasis on Impurity Effects *J. Phys. Chem. Solids* <u>30</u>, 551-564 (1969).

28. Harrick, N. J., *Internal Reflection Spectroscopy*, (J. Wiley and Sons, New York, 1967).

29. Holm, R. T., and Palik, E. D., Thin Film Adsorption Coefficients by Attenuated-Total-Reflection Spectroscopy, *Appl. Opt.* <u>17</u>, 394-403 (1978).

30. Hass, M., Davisson, J. W., Rosenstock, H. B., and Babiskin, J., Measurement of Very Low Adsorption Coefficients by Laser Calorimetry, *Appl. Opt.* <u>14</u>, 1128-1130 (1975).

31. Moravec, T. J., and Bernal, E. G., Automation of a Laser Absorption Calorimeter, *Appl. Opt.* <u>17</u>, 1938-1942 (1978).

32. Allred, D. D., White, C. W., Clark, G. J., Appleton, B. R., and Tsong, I. S. T., Measurement of Hydrogen Profiles in SiO₂ by a Nuclear Reaction Technique, *The Physics of SiO₂ and Its Interfaces*, S. T. Pantelides, Ed, pp. 210-214 (Pergamon Press, New York, 1978).

Table 1. Water-Induced Reactions During Oxidation of Silicon at 1300 K.

Reactions	K
$Si(c) + 2H_2O(g) \rightleftarrows SiO_2(c) + 2H_2(g)$	1.33×10^{13}
$Si(c) + \frac{7}{2}H_2O(g) \rightleftarrows \frac{1}{2}SiO_2(OH)_6(g) + 2H_2(g)$	1.87×10^6
$Si(c) + 3H_2O(g) \rightleftarrows SiO(OH)_2(g) + 2H_2(g)$	1.31×10^6
$Si(c) + 2H_2O(g) \rightleftarrows SiO(OH)(g) + \frac{3}{2}H_2(g)$	5.20×10^3
$Si(c) + H_2O(g) \rightleftarrows \frac{1}{2}SiO_2(c) + \frac{1}{2}SiH_4(g)$	3.78×10^3
$\frac{1}{2}Si(c) + 2H_2O(g) \rightleftarrows \frac{1}{2}Si(OH)_4(g) + H_2(g)$	2.75×10^2
$Si(c) + H_2O(g) \rightleftarrows SiO(g) + H_2(g)$	27.56
$Si(c) + OH(g) \rightleftarrows SiOH(g)$	1.61×10^2
$Si(c) + H_2O(g) \rightleftarrows SiOH(g) + \frac{1}{2}H_2(g)$	2.29×10^{-6}
$Si(c) + H_2O(g) \rightleftarrows SiOH(g) + H(g)$	2.52×10^{-12}
$SiO_2(c) + \frac{1}{2}H_2O(g) \rightleftarrows SiO(OH)(g) + \frac{1}{4}O_2(g)$	1.15×10^{-13}
$SiO_2(c) + \frac{3}{2}H_2O(g) \rightleftarrows Si(OH)_3(g) + \frac{1}{4}O_2(g)$	6.81×10^{-18}
$Si(c) + \frac{1}{2}O_2(g) \rightleftarrows SiO(g)$	3.20×10^8
$Si(c) + O_2(g) \rightleftarrows SiO_2(g)$	2.51×10^{12}
$Si(c) + O_2(g) \rightleftarrows SiO_2(c)$	1.8×10^{27}
$Si(c) + O_2(g) + H_2O(g) \rightleftarrows SiO(OH)(g) + OH(g)$	2.71×10^{10}
$Si(c) + O_2(g) + H_2O(g) \rightleftarrows Si(OH)(g) + \frac{1}{2}O_2(g)$	3.28×10^{10}
$Si(c) + O_2(g) + H_2O(g) \rightleftarrows SiO(OH)_2(g)$	6.21×10^{20}
$Si(c) + O_2(g) + 2H_2O(g) \rightleftarrows Si(OH)_4(g)$	3.59×10^{19}
$Si(c) + O_2(g) + \frac{3}{2}H_2O(g) \rightleftarrows \frac{1}{2}Si_2O(OH)_6(g)$	8.54×10^{20}
$SiO(g) + \frac{1}{2}O_2(g) \rightleftarrows SiO_2(c)$	5.59×10^{18}
$SiO(g) + \frac{1}{2}O_2(g) \rightleftarrows SiO_2(g)$	7.86×10^3
$SiO(g) + H_2O(g) \rightleftarrows SiO(OH)(g) + \frac{1}{2}H_2(g)$	5.16×10^2
$SiO(g) + 2H_2O(g) \rightleftarrows SiO(OH)_2(g) + H_2(g)$	1.67×10^5
$SiO(g) + 3H_2O(g) \rightleftarrows Si(OH)_4(g) + H_2(g)$	9.69×10^3
$SiO(g) + \frac{5}{2}H_2O(g) \rightleftarrows \frac{1}{2}Si_2O(OH)_6(g) + H_2(g)$	2.30×10^5

Table 2. Thermodynamic Data Used to Calculate Equilibrium
Constants at 1300 K for Reactions Listed in Table 1.

Compound	ΔH°_{f298} (kcal/mole)	$-(G^\circ_T - H_{298})/T$ (cal/K·mole)
$H_2O(g)$	-57.798	51.136
$H(g)$	52.1	30.879
$OH(g)$	9.432	48.877
$O(g)$	59.559	42.044
$O_2(g)$	0.0	54.283
$H_2(g)$	0.0	36.130
$SiO_2(c)$	-217.7	19.918
$SiO_2(l)$	-215.74	21.134
$SiO_2(g)$	-73.0	63.266
$SiO(g)$	-24.0	55.994
$Si(c)$	0.0	8.399
$Si(l)$	11.585	15.188
$Si(g)$	107.7	43.715
$SiH(g)$	90.0	52.515
$SiH_4(g)$	7.3	58.969
$SiO(OH)(g)$	-118.0	71.63*
$Si(OH)_2(g)$	-101.0	72.42*
$SiO(OH)_2(g)$	-222.0	80.15*
$Si(OH)_4(g)$	-322.3	92.93*
$SiO_2(OH)_6(g)$	-612.1	128.83*
$Si(OH)(g)$	4.0	63.2
$Si(OH)_3(g)$	-203.0	82.5

*These data replace corresponding data in
Reference [2]. The effect on the results
given there is small and the conclusions
are unchanged.

Table 3. Water Fluence (F) on Wafer Unit Area During the Oxidation Period (t) Necessary to Grow 100-nm Silicon Dioxide on <100> Silicon. The oxidation atmosphere (1 atm oxygen) contains 1 ppm or 125 ppm water.

T (°C)	T (K)	$\rho(H_2O)$ (cm⁻³)	k_L^* (nm/min) $P(H_2O) = 10^{-6}$ atm	k_P^* (nm²/min)	t (min)	F (cm⁻²)	$\rho(H_2O)$ (cm⁻³)	k_L^* (nm/min)	k_P^* (nm²/min) $P(H_2O) = 125 \times 10^{-6}$ atm	t (min)	F (cm⁻²)
780	1053	6.97×10^{12}	0.057	2.65	5343	6.21×10^{22}	8.71×10^{14}	0.065	2.85	4878	7.09×10^{24}
800	1073	6.84×10^{12}	0.073	5.2	3189	3.67×10^{22}	8.55×10^{14}	0.08	6.3	2750	3.96×10^{24}
893	1166	6.29×10^{12}	0.22	42.5	671	7.41×10^{21}	7.87×10^{14}	0.23	65	574	7.93×10^{23}
900	1173	6.26×10^{12}	0.235	46.8	622	6.86×10^{21}	7.82×10^{14}	0.255	72	518	7.13×10^{23}
980	1253	5.86×10^{12}	0.77	140	196	2.09×10^{21}	7.32×10^{14}	0.84	193	166	2.21×10^{23}
1000	1273	5.77×10^{12}	0.87	153	175	1.85×10^{21}	7.20×10^{14}	0.965	205	148	1.95×10^{23}
1100	1373	5.35×10^{12}	3.1	350	59	6.01×10^{20}	6.68×10^{14}	3.4	475	49	6.24×10^{22}
1200	1473	4.98×10^{12}	10.8	640	24	2.35×10^{20}	6.23×10^{14}	12.1	860	19	2.34×10^{22}

* Reference [18].

Table 4. Water Permeation Through 0.1-cm Thick Fused Silica. Room ambient at 25°C with 30-percent relative humidity [$P(H_2O) = 9.4 \times 10^{-3}$ atm].

T (°C)	T (K)	$D_{in}(OH)$ (*) (cm² s⁻¹)	$D_{out}(OH)$ (*) (cm² s⁻¹)	$C(OH)$ (*) cm⁻³	$D_{out}\frac{\delta C}{\delta x}$ (cm⁻² s⁻¹)	$\bar{v}(OH)$ (cm s⁻¹)	$\bar{v}(O_2)$ (cm s⁻¹)	$n(O_2)$	$D(OH-O_2)$ (cm² s⁻¹)	z_r (cm)	$\rho(OH)$ cm⁻³	$P(OH)$ (atm)
800	1073	1.9×10^{-10}	0.81×10^{-10}	9.4×10^{18}	7.6×10^{9}	1.12×10^{5}	8.4×10^{4}	6.82×10^{18}	1.3	1.61	4.7×10^{9}	6.9×10^{-10}
900	1173	3.9×10^{-10}	1.6×10^{-10}	8.1×10^{18}	1.3×10^{10}	1.17×10^{5}	8.8×10^{4}	6.23×10^{18}	1.48	1.72	7.6×10^{9}	1.2×10^{-9}
1000	1273	7.2×10^{-10}	2.9×10^{-10}	7.0×10^{18}	2.0×10^{10}	1.22×10^{5}	9.17×10^{4}	5.73×10^{18}	1.68	1.83	1.1×10^{10}	1.9×10^{-9}
1100	1373	1.2×10^{-9}	4.8×10^{-10}	6.8×10^{18}	3.3×10^{10}	1.27×10^{5}	9.53×10^{4}	5.33×10^{18}	1.88	1.94	1.7×10^{10}	3.2×10^{-9}
1200	1473	1.9×10^{-9}	7.3×10^{-10}	6.3×10^{18}	4.6×10^{10}	1.31×10^{5}	9.86×10^{4}	4.97×10^{18}	2.08	2.04	2.2×10^{10}	4.4×10^{-9}

(*) Data calculated from References [20,21] for $P(H_2O) = 9.4 \times 10^{-3}$ atm.

Table 5. Si-OH and Si-H Bond Energies for
Various Silicon Compound Molecules.

Compound	Type	Bond Energy (kcal/mole)	Bond Energy (eV/molecule)
$SiO(g)$	$Si = O$	190	8.24
$SiO_2(g)$	$Si = O$	149	6.46
$Si(OH)_3(g)$	$Si-OH$	127	5.51
$Si_2O(OH)_6(g)$	$Si-OH$	117.5	5.10
$Si(OH)_4(g)$	$Si-OH$	116.5	5.05
$SiO(OH)g$	$Si-OH$	113	4.90
$SiH_4(g)$	$Si-H$	76	3.30
$SiH(g)$	$Si-H$	73.5	3.19
$Si_2H_6(g)$	$Si-Si$	51	2.21
$Si_3H_8(g)$	$Si-Si$		
	$O-H$	102.2	4.43
	$O-H\cdots O$	~ 5	~ 0.22
	$Si = Si$	75.8	3.29
	$Si-Si$	53.4	2.32
	$Si-O$	111	4.82
	$Si = O$	192.3	8.34
	$O = O$	119.2	5.17
	$O-O$	34.0	1.48
	$O-H$	110.8	4.81
	$Si-H$	74.7	3.24
	$Si \equiv Si$	153.6	6.66

Director
Armed Forces Radiobiology Research Institute
Defense Nuclear Agency
National Naval Medical Center
Bethesda, MD 20014
    ATTN Technical Library

Commander in Chief
U.S. European Command, JCS
APO New York 09128
    ATTN ECJ6-PF

Defense Communication Engineer Center
1860 Wiehle Avenue
Reston, VA 22090
    ATTN R410 James W. McLean
    ATTN R320 C. W. Bergman

Director
Defense Communications Agency
Washington, DC 20305
    ATTN 930 Monte I. Burgett, Jr.

Defense Documentation Center
Cameron Station
Alexandria, VA 22314
    ATTN TC

Director
Defense Intelligence Agency
Washington, DC 20301
    ATTN DS-4A2

Director
Defense Nuclear Agency
Washington, DC 20305
    ATTN STVL
    ATTN RAEV
    ATTN DDST
    ATTN TITL Tech Library

Commander
Field Command
Defense Nuclear Agency
Kirtland AFB, NM 87115
    ATTN FCPR

Director
Interservice Nuclear Weapons School
Kirtland AFB, NM 87115
    ATTN Document Control

Director
Joint Strat TGT Planning Staff JCS
Offutt AFB
Omaha, NE 68113
    ATTN JLTW-2

Chief
Livermore Division Fld Command DNA
Lawrence Livermore Laboratory
P.O. Box 808
Livermore, CA 94550
    ATTN FCPRL

Director
National Security Agency
Ft. George G. Meade, MD 20755
    ATTN Orland O. Van Gunten R-425
    ATTN TDL

OJCS/J-3
The Pentagon
Washington, DC 20301
    ATTN J-3 RDTA BR WWMCCS Plans Div

Under Secretary of Defense for Rsch & Engrg
Department of Defense
Washington, DC 20301
    ATTN S&SS (OS)

Project Manager
Army Tactical Data Systems
U.S. Army Electronics Command
Fort Monmouth, NJ 07703
    ATTN DRCPN-TDS-SD
    ATTN Dwaine B. Huewe

Commander
BMD System Command
P.O. Box 1500
Huntsville, AL 35807
    ATTN BDMSC-TEN

Commander
Frankford Arsenal
Bridge and Tacony Streets
Philadelphia, PA 19137
    ATTN SARFA-FCD

Commander
Harry Diamond Laboratories
2800 Powder Mill Road
Adelphi, MD 20783
    ATTN DRXDO-EM (2)
    ATTN DRXDO-NP
    ATTN DRXDO-RB
    ATTN DRXDO-TF
    ATTN DRXDO-RCC
    ATTN DRXDO-TI Tech Library
    ATTN J. McGarrity

Commanding Officer
Night Vision Laboratory
U.S. Army Electronics Command
Fort Belvoir, VA 22060
    ATTN Capt. Allan S. Parker

Commander
Picatinny Arsenal
Dover, NJ 07801
    ATTN SARPA-ND-C-E
    ATTN SMUPA-ND-N-E
    ATTN SMUPA-FR-S-P (2)
    ATTN SARPA-ND-N
    ATTN SMUPA-ND-D-B
    ATTN SMUPA-ND-W
    ATTN SARPA-FR-E

Commander
Redstone Scientific Information Center
U.S. Army Missile Command
Redstone Arsenal, AL 35809
    ATTN Chief, Documents

Secretary of the Army
Washington, DC 20310
    ATTN ODUSA or Daniel Willard

Director
TRASANA
White Sands Missile Range, NM 88002
    ATTN ATAA-EAC

Director
U.S. Army Ballistic Research Labs
Aberdeen Proving Ground, MD 21005
    ATTN DRXBR-X
    ATTN DRXBR-VL (2)
    ATTN DRXBR-AM
    ATTN DRXRD-BVL

Chief
U.S. Army Communications Sys. Agency
Fort Monmouth, NJ 07703
    ATTN SCCM-AD-SV Library

Commander
U.S. Army Electronics Command
Fort Monmouth, NJ 07703
    ATTN DRSEL-TL-IR
    ATTN DRSEL-CE-T
    ATTN DRSEL-CT-HDK
    ATTN DRSEL-GG-TD
    ATTN DRSEL-TL-MD
    ATTN DRSEL-TL-ND
    ATTN DRSEL-PL-ENV

Commander
U.S. Army Electronics Proving Ground
Fort Huachuca, AZ 85613
    ATTN STEEP-MT-M

Commandant
U.S. Army Engineer School
Fort Belvoir, VA 22060
    ATTN ATSE-CTD-CS

Commander-in-Chief
U.S. Army Europe and Seventh Army
APO New York 09403 (Heidelberg)
    ATTN ODCSE-E AEAGE-PI

Commandant
U.S. Army Field Artillery School
Fort Sill, OK 73503
    ATTN ATSFA-CTD-ME

Commander
U.S. Army Mat & Mechanics Rsch Center
Watertown, MA 02172
    ATTN DRXMR-HH

Commander
U.S. Army Materiel Dev. & Readiness Cmd.
5001 Eisenhower Avenue
Alexandria, VA 22333
    ATTN DRCDE-D

Commander
U.S. Army Missile Command
Redstone Arsenal, AL 35809
    ATTN DRSI-RGP
    ATTN DRCPM-PE-EA
    ATTN DRSMI-RGP
    ATTN DRSMI-TRA

Chief
U.S. Army Nuc. and Chemical Surety Group
Bldg. 2073, North Area
Fort Belvoir, VA 22060
    ATTN MOSG-ND

Commander
U.S. Army Nuclear Agency
7500 Backlick Road
Building 2073
Springfield, VA 22150
    ATTN ATCN-W

Commander
U.S. Army Tank Automotive Command
Warren, MI 48090
    ATTN DRCPM-GCM-SW

Commander
U.S. Army Test and Evaluation Command
Aberdeen Proving Ground, MD 21005
    ATTN DRSTE-EL
    ATTN DRSTE-NB

Commander
White Sands Missile Range
White Sands Missile Range, NM 88002
    ATTN STEWS-TE-NT

Chief of Naval Research
Navy Department
Arlington, VA 22217
    ATTN 427

Commanding Officer
Naval Avionics Facility
21st and Arlington Avenue
Indianapolis, IN 46218
    ATTN 942

Commander
Naval Electronic Systems Command
Naval Electronic Systems Cmd Hqs
Washington, DC 20360
    ATTN 50451?
    ATTN 5032
    ATTN PME 117-21
    ATTN 50451
    ATTN ELEX 05323

Commanding Officer
Naval Intelligence Support Center
4301 Suitland Road, Bldg. 5
Washington, DC 20390
    ATTN NISC-45

Commander
Naval Ocean Systems Center
San Diego, CA 92152
    ATTN H. F. Wong

Director
Naval Research Laboratory
Washington, DC 20375
    ATTN 5210
    ATTN 5216
    ATTN 6631
    ATTN 6440
    ATTN 601 E. Wolicki
    ATTN 4104
    ATTN 7701
    ATTN 2627

Commander
Naval Sea Systems Command
Navy Department
Washington, DC 20362
    ATTN SEA-9931 (2)

Officer-in-Charge
Navay Surface Weapons Center
White Oak, Silver Spring, MD 20910
    ATTN WA501 Navy Nuc. Prgms Off.
    ATTN WA50
    ATTN WA52

Commander
Naval Surface Weapons Center
Dahlgren Laboratory
Dahlgren, VA 22448
    ATTN FUR Robert A. Amadori

Commander
Naval Weapons Center
China Lake, CA 93555
    ATTN 533 Tech Library

Commanding Officer
Naval Weapons Evaluation Facility
Kirtland AFB
Albuquerque, NM 87117
    ATTN ATG Mr. Stanley

Commanding Officer
Naval Weapons Support Center
Crane, IN 47522
    ATTN 70242
    ATTN 7024

Commanding Officer
Nuclear Weapons Tng. Center Pacific
Naval Air Station, North Island
San Diego, CA 92135
    ATTN 50

Director
Strategic Systems Project Office
Navy Department
Washington, DC 20376
    ATTN NSP-27331
    ATTN NSP-2342
    ATTN SP 2701

AF Aero-Propulsion Laboratory, AFSC
Wright-Patterson AFB, OH 45433
    ATTN POD P. E. Stover

AF Geophysics Laboratory, AFSC
Hanscom AFB, MA 01731
    ATTN LQR Edward A. Burke
    ATTN J. Emery Cormier
    ATTN LGD-Stop 30 Freeman Shepherd

AF Institute of Technology, AU
Wright-Patterson AFB, OH 45433
    ATTN ENP Charles J. Bridgman

AF Materials Laboratory, AFSC
Wright-Patterson AFB, OH 45433
    ATTN LTE

26

AF Weapons Laboratory, AFSC
Kirtland AFB, NM 87117
       ATTN DEX
       ATTN ELA
       ATTN NTS
       ATTN ELP Tree Section
       ATTN NT Carl E. Baum
       ATTN ELS
       ATTN ELXT

AFTAC
Patrick AFB, FL 32925
       ATTN TAE
       ATTN TFS Maj. Marion F. Schneider

Air Force Avionics Laboratory, AFSC
Wright-Patterson AFB, OH 45433
       ATTN AAT Mason Friar
       ATTN DHM C. Friend
       ATTN DH LtC. McKenzie
       ATTN DHE H. J. Hennecke

Commander
ASD
Wright-Patterson AFB, OH 45433
       ATTN ASD/ENESS
       ATTN ASD-YH-EX
       ATTN ENACC Robert L. Fish

Headquarters
Electronic Systems Division/YS
Hanscom AFB, MA 01731
       ATTN YSEV

Headquarters
Electronic Systems Division/YW
Hanscom AFB, MA 01731
       ATTN YWEI

Commander
Foreign Technology Division, AFSC
Wright-Patterson AFB, OH 45433
       ATTN ETD/PDJC
       ATTN ETDP

Commander
Ogden Air Logistics Center
Hill AFB, UT 84401
       ATTN MMEWM

Commander
Rome Air Development Center, AFSC
Griffiss AFB, NY 13440
       ATTN RBRAC
       ATTN RBRP

Commander
Rome Air Development Center, AFSC
Hanscom AFB, MA 01731
       ATTN ETS
       ATTN ET R. Buchanan

SAMSO/DY
P.O. Box 92960
Worldway Postal Center
Los Angeles, CA 90009
       ATTN DYS

SAMSO/IN
P.O. Box 92960
Worldway Postal Center
Los Angeles, CA 90009
       ATTN IND I. J. Judy

SAMSO/MN
Norton AFB, CA 92409
       ATTN MNNH

SAMSO/RS
P.O. Box 92960
Worldway Postal Center
Los Angeles, CA 90009
       ATTN RSSE
       ATTN RSMG

SAMSO/SK
P.O. Box 92960
Worldway Postal Center
Los Angeles, CA 90009
       ATTN SKF

SAMSO/SZ
P.O. Box 92960
Worldway Postal Center
Los Angeles, CA 90009
       ATTN SZJ

Commander in Chief
Strategic Air Command
Offutt AFB, NB 68113
       ATTN NRI-STINFO Library
       ATTN XPFS

Department of Energy
Albuquerque Operations Office
P.O. Box 5400
Albuquerque, NM 87115
       ATTN Document Control for WSSB

University of California
Lawrence Livermore Laboratory
P.O. Box 808
Livermore CA 94550
    ATTN Lawrence Cleland L-156
    ATTN E. K. Miller L-156
    ATTN Frederick R. Kovar L-31 (Class L-94)
    ATTN Joseph E. Keller, Jr. L-125
    ATTN Hans Kruger L-96 (Class L-94)
    ATTN Tech. Info. Dept. L-3
    ATTN Ronald L. Ott L-531
    ATTN William J. Hogan L-389
    ATTN Donald J. Meeker L-545 (Class L-153)

Los Alamos Scientific Laboratory
P.O. Box 1663
Los Alamos, NM 87545
    ATTN DOC CON for J. Arthur Freed
    ATTN DOC CON for Bruce W. Noel

Sandia Laboratories
P.O. Box 5800
Albuquerque, NM 87115
    ATTN DOC CON for R. Gregory ORG 2140
    ATTN DOC CON for 3141 Sandia Rpt Coll
    ATTN DOC CON for J. A. Hood ORG 2110

Department of Commerce
National Bureau of Standards
Washington, DC 20234
    ATTN Judson C. French

Aerojet Electro-Systems Co.
Div. of Aerojet-General Corporation
P.O. Box 296, 1100 W. Hollyvale Drive
Azusa, CA 91702
    ATTN Thomas D. Hanscome

Aerospace Corporation
P.O. Box 92957
Los Angeles, CA 90009
    ATTN John Ditre
    ATTN Irving M. Garfunkel
    ATTN S. P. Bower
    ATTN Library
    ATTN L. W. Aukerman
    ATTN Julian Reinheimer
    ATTN William W. Willis

Analog Technology Corporation
3410 East Foothill Boulevard
Pasadena, CA 91107
    ATTN John Joseph Baum

AVCO Research & Systems Group
201 Lowell Street
Wilmington, MA 01887
    ATTN Research Lib. A830 Rm 7201

BDM Corporation, The
7915 Jones Branch Drive
McLean, VA 22101
    ATTN T. H. Neighbors

BDM Corporation, The
P.O. Box 9274
Albuquerque International
Albuquerque, NM 87119
    ATTN D. R. Alexander

Bendix Corporation, The
Communication Division
East Joppa Road
Baltimore, MD 21204
    ATTN Document Control

Bendix Corporation, The
Research Laboratories Division
Bendix Center
Southfield, MI 48075
    ATTN Mgr Prgm Dev Donald J. Niehaus
    ATTN Max Frank

Boeing Company, The
P.O. Box 3707
Seattle, WA 98124
    ATTN Howard W. Wicklein MS 17-11
    ATTN Aerospace Library
    ATTN Donald W. Egelkrout MS 2R-00
    ATTN Itsu Amura
    ATTN Robert S. Caldwell 2R-00
    ATTN Carl Rosenberg 2R-00

Booz-Allen and Hamilton, Inc.
106 Apple Street
Tinton Falls, NJ 07724
    ATTN Raymond J. Chrisner

California Institute of Technology
Jet Propulsion Laboratory
4800 Oak Grove Drive
Pasadena, CA 91103
    ATTN J. Bryden
    ATTN A. G. Stanley

Charles Stark Draper Laboratory, Inc.
555 Technology Square
Cambridge, MA 02139
    ATTN Paul R. Kelly
    ATTN Kenneth Fertig

Cincinnati Electronics Corporation
2630 Glendale-Milford Road
Cincinnati, OH 45241
    ATTN C. R. Stump
    ATTN Lois Hammond

Control Data Corporation
P.O. Box 0
Minneapolis, MN 55440
    ATTN Jack Meehan

Cutler-Hammer, Inc.
AIL Division
Comack Road
Deer Park, NY 11729
    ATTN Central Tech Files Anne Anthony

Denver, University of
Colorado Seminary
Denver Research Institute
P.O. Box 10127
Denver, CO 80210
    ATTN Sec. Officer for Fred P. Venditti

Dikewood Industries, Inc.
1009 Bradbury Drive, S.E.
Albuquerque, NM 87106
    ATTN L. Wayne Davis

E-Systems, Inc.
Greenville Division
P.O. Box 1056
Greenville, TX 75401
    ATTN Library 8-50100

Effects Technology, Inc.
5383 Hollister Avenue
Santa Barbara, CA 93111
    ATTN Edward John Steele

Exp & Math Physics Consultants
P.O. Box 66331
Los Angeles, CA 90066
    ATTN Thomas M. Jordan

Fairchild Camera and Instrument Corp
464 Ellis Street
Mountain View, CA 94040
    ATTN Sec. Dept for 2-233 David K. Myers

Fairchild Industries, Inc.
Sherman Fairchild Technology Center
20301 Century Boulevard
Germantown, MD 20767
    ATTN Mgr Config Data & Standards

Florida, University of
An Institution of Education
ATTN: Patricia B. Rambo
P.O. Box 284
Gainesville, FL 32601
    ATTN D. P. Kennedy

Ford Aerospace & Communications Corp.
3939 Fabian Way
Palo Alto, CA 94303
    ATTN Edward R. Hahn MS-X22
    ATTN Donald R. McMorrow MS G30
    ATTN Samuel R. Crawford MS 531

Ford Aerospace & Communications Operations
Ford & Jamboree Roads
Newport Beach, CA 92663
    ATTN Ken C. Attinger
    ATTN E. R. Poncelet, Jr.
    ATTN Tech Info Section

Franklin Institute, The
20th Street and Parkway
Philadelphia, PA 19103
    ATTN Ramie H. Thompson

Garrett Corporation
P.O. Box 92248, 9851 Sepulveda Blvd.
Los Angeles, CA 90009
    ATTN Robert E. Weir Dept 93-9

General Dynamics Corp.
Electronics Div. Orlando Operations
P.O. Box 2566
Orlando, FL 32802
    ATTN D. W. Coleman

General Electric Company
Space Division
Valley Forge Space Center
Goddard Blvd, King of Prussia
P.O. Box 8555
Philadelphia, PA 19101
    ATTN John L. Andrews
    ATTN Joseph C. Peden VFSC. Rm 4230M
    ATTN Larry I. Chasen

General Electric Company
Re-entry & Environmental Systems Div
P.O. Box 7722
3198 Chestnut Street
Philadelphia, PA 19101
    ATTN Robert V. Benedict
    ATTN John W. Palchefsky, Jr.

General Electric Company
Ordnance Systems
100 Plastics Avenue
Pittsfield, MA 01201
    ATTN Joseph J. Reidl

General Electric Company
Tempo-Center for Advanced Studies
816 State Street (P.O. Drawer QQ)
Santa Barbara, CA 93102
        ATTN William McNamera
        ATTN M. Espig
        ATTN Royden R. Rutherford
        ATTN DASIAC

General Electric Company
Aircraft Engine Business Group
Evendale Plant Int Hwy 75 S
Cincinnati, OH 45215
        ATTN John A. Ellerhorst E 2

General Electric Company
Aerospace Electronics Systems
French Road
Utica, NY 13503
        ATTN W. J. Patterson Drop 233
        ATTN Charles M. Hewison Drop 624

General Electric Company
P.O. Box 5000
Binghamton, NY 13902
        ATTN David W. Pepin Drop 160

General Electric Company-Tempo
ATTN: DASIAC
c/o Defense Nuclear Agency
Washington, DC 20305
        ATTN William Alfonte

General Research Corporation
P.O. Box 3587
Santa Barbara, CA 93105
        ATTN Robert D. Hill

Georgia Institute of Technology
Georgia Tech Research Institute
Atlanta, GA 30332
        ATTN R. Curry (uncl only)

Grumman Aerospace Corporation
South Oyster Bay Road
Bethpage, NY 11714
        ATTN Jerry Rogers Dept 533

GTE Sylvania, Inc.
Electronics Systems Grp-Eastern Div
77 A Street
Needham, MA 02194
        ATTN James A. Waldon
        ATTN Charles A. Thornhill Librarian
        ATTN Leonard L. Blaisdell

GTE Sylvania, Inc.
189 B Street
Needham Heights, MA 02194
        ATTN H & V Group
        ATTN Paul B. Frederickson
        ATTN Herbert A. Ullman
        ATTN Charles H. Ramsbottom

Gulton Industries, Inc.
Engineered Magnetics Division
13041 Cerise Avenue
Hawthorne, CA 90250
        ATTN Engnmagnetics Div

Harris Corporation
Harris Semiconductor Division
P.O. Box 883
Melbourne, FL 32901
        ATTN Carl F. Davis MS 17-220
        ATTN Wayne E. Abare MS 16-111
        ATTN T. L. Clark MS 4040

Hazeltine Corporation
Pulaski Road
Greenlawn, NY 11740
        ATTN Tech Info Ctr M. Waite

Honeywell Incorporated
Avionics Division
2600 Ridgeway Parkway
Minneapolis, MN 55413
        ATTN Ronald R. Johnson A1622
        ATTN R. J. Kell MS S2572

Honeywell Incorporated
Avionics Division
13350 U.S. Highway 19 North
St. Petersburg, FL 33733
        ATTN Harrison H. Noble MS 725-5A
        ATTN Stacey H. Graff MS 725-5

Honeywell Incorporated
Radiation Center
2 Forbes Road
Lexington, MA 02173
        ATTN Technical Library

Hughes Aircraft Company
Centinela and Teale
Culver City, CA 90230
        ATTN John B. Singletary MS 6-D133
        ATTN Dan Binder MS 6-D147
        ATTN Kenneth R. Walker MS D157
        ATTN Billy W. Campbell MS 6-E110

Hughes Aircraft Company, El Segundo Site
P.O. Box 92919
Los Angeles, CA 90009
        ATTN Edward C. Smith MS A620
        ATTN William W. Scott MS A1080

IBM Corporation
Route 17C
Owego, NY 13827
    ATTN Harry W. Mathers Dept M41
    ATTN Frank Frankovsky

IIT Research Institute
10 West 35th Street
Chicago, IL 60616
    ATTN Irving N. Mindel

Intl. Tel. & Telegraph Corporation
500 Washington Avenue
Nutley, NJ 07110
    ATTN Alexander T. Richardson

Ion Physics Corporation
South Bedford Street
Burlington, MA 01803
    ATTN Robert D. Evans

IRT Corporation
P.O. Box 81087
San Diego, CA 92138
    ATTN Leo D. Cotter
    ATTN MDC
    ATTN R. L. Mertz

JAYCOR
1401 Camino Del Mar
Del Mar, CA 92014
    ATTN Eric P. Wenaas

JAYCOR
205 S. Whiting Street, Suite 500
Alexandria, VA 22304
    ATTN Robert Sullivan
    ATTN Catherine Turesko

Johns Hopkins University
Applied Physics Laboratory
Johns Hopkins Road
Laurel, MD 20810
    ATTN Peter E. Partridge

Kaman Sciences Corporation
P.O. Box 7463
Colorado Springs, CO 80933
    ATTN Donald H. Bryce
    ATTN Albert P. Bridges
    ATTN John R. Hoffman
    ATTN Jerry I. Lubell
    ATTN W. Foster Rich
    ATTN Walter E. Ware

Litton Systems, Inc.
Guidance & Control Systems Division
5500 Canoga Avenue
Woodland Hills, CA 91364
    ATTN Val J. Ashby MS 67
    ATTN John P. Retzler
    ATTN R. W. Maughmer

Litton Systems, Inc.
Electron Tube Division
1035 Westminster Drive
Williamsport, PA 17701
    ATTN Frank J. McCarthy

Lockheed Missiles & Space Co., Inc.
P.O. Box 504
Sunnyvale, CA 94088
    ATTN Samuel I. Taimuty, Dept 85-85
    ATTN L. Rossi, Dept 81-64
    ATTN Benjamin T. Kimura, Dept.81-14
    ATTN Edwin A. Smith, Dept 85-85
    ATTN George F. Heath, Dept 81-14

Lockheed Missiles and Space Co., Inc.
3251 Hanover Street
Palo Alto, CA 94304
    ATTN Tech Info Ctr D/Coll

M.I.T. Lincoln Laboratory
P.O. Box 73
Lexington, MA 02173
    ATTN Leona Loughlin Librarian A-082

Martin Marietta Corporation
Orlando Division
P.O. Box 5837
Orlando, FL 32805
    ATTN Mona C. Griffith Lib MP-30
    ATTN William W. Mras MP-413
    ATTN Jack M. Ashford MP-537

Martin Marietta Corporation
Denver Division
P.O. Box 179
Denver, CO 80201
    ATTN Ben T. Graham MS PO-454
    ATTN Research Lib 6617 Jay R. McKee
    ATTN J. E. Goodwin Mail 0452
    ATTN Paul G. Kase Mail 8203

McDonnell Douglas Corporation
P.O. Box 516
St. Louis, Missouri 63166
    ATTN Tom Ender
    ATTN Technical Library

McDonnell Douglas Corporation
5301 Bolsa Avenue
Huntington Beach, CA 92647
    ATTN Stanley Schneider

McDonnell Douglas Corporation
3855 Lakewood Boulevard
Long Beach, CA 90846
    ATTN Technical Library, C1-290/36-84

Mission Research Corporation
735 State Street
Santa Barbara, CA 93101
    ATTN William C. Hart

Mission Research Corporation
P.O. Box 8693, Station C
Albuquerque, NM 87108
    ATTN David E. Merewether

Mission Research Corporation - San Diego
P.O. Box 1209
La Jolla, CA 92038
    ATTN J. P. Raymond
    ATTN V. A. J. Van Lint

Mitre Corporation, The
P.O. Box 208
Bedford, MA 01730
    ATTN M. E. Fitzgerald
    ATTN Library

National Academy of Sciences
ATTN: National Materials Advisory Board
2101 Constitution Avenue, NW
Washington, DC 20418
    ATTN R. S. Shane Nat Materials Advsy

New Mexico, University of
Electrical Engineering & Computer Science Dept
Albuquerque, NM 87131
    ATTN Harold Southward

Northrop Corporation
Electronic Division
1 Research Park
Palos Verdes Peninsula, CA 90274
    ATTN George H. Towner
    ATTN Boyce T. Ahlport

Northrop Corporation
Northrop Research and Technology Ctr
3401 West Broadway
Hawthorne, CA 90250
    ATTN Orlie L. Curtis, Jr.
    ATTN J. R. Srour
    ATTN David N. Pocock

Northrop Corporation
Electronic Division
2301 West 120th Street
Hawthorne, CA 90250
    ATTN Joseph D. Russo
    ATTN John M. Reynolds
    ATTN Vincent R. DeMartino

Palisades Inst for Research Services, Inc.
201 Varick Street
New York, NY 10014
    ATTN Records Supervisor

Physics International Company
2700 Merced Street
San Leandro, CA 94577
    ATTN Doc Con for Charles H. Stallings
    ATTN Doc Con for John H. Huntington

R & D Associates
P.O. Box 9695
Marina Del Rey, CA 90291
    ATTN S. Clay Rogers

Rand Corporation, The
1700 Main Street
Santa Monica, CA 90406
    ATTN Cullen Crain

Raytheon Company
Hartwell Road
Bedford, MA 01730
    ATTN Gajanan H. Joshi Radar Sys Lab

Raytheon Company
528 Boston Post Road
Sudbury, MA 01776
    ATTN Harold L. Flescher

RCA Corporation
Government Systems Division
Astro Electronics
P.O. Box 800, Locust Corner
East Windsor Township
Princeton, NJ 08540
    ATTN George J. Brucker

RCA Corporation
Camden Complex
Front & Cooper Streets
Camden, NJ 08012
    ATTN E. Van Keuren 13-5-2

Rensselaer Polytechnic Institute
P.O. Box 965
Troy, NJ 12181
    ATTN Ronald J. Gutmann

Research Triangle Institute
P.O. Box 12194
Research Triangle Park, NC 27709
    ATTN Sec Officer for
    ATTN Eng Div Mayrant Simons, Jr.

Rockwell International Corporation
P.O. Box 3105
Anaheim, CA 92803
    ATTN George C. Messenger FB61
    ATTN Donald J. Stevens FA70
    ATTN K. F. Hull
    ATTN James E. Bell HA10
    ATTN N. J. Rudie FA53

Rockwell International Corporation
5701 West Imperial Highway
Los Angeles, CA 90009
    ATTN T. B. Yates

Rockwell International Corporation
Collins Divisions
400 Collins Road NE
Cedar Rapids, IA 52406
    ATTN Mildred A. Blair
    ATTN Dennis Sutherland
    ATTN Alan A. Langenfeld

Sanders Associates, Inc.
95 Canal Street
Nashua, NH 03060
    ATTN Moe L. Aitel NCA 1-3236

Science Applications, Inc.
P.O. Box 277
Berkeley, CA 94701
    ATTN Frederick M. Tesche

Science Applications, Inc.
P.O. Box 2351
La Jolla, CA 92038
    ATTN J. Robert Beyster
    ATTN Larry Scott

Science Applications, Inc.
Huntsville Division
2109 W. Clinton Avenue
Suite 700
Huntsville, AL 35805
    ATTN Noel R. Byrn

Science Applications, Inc.
P.O. Box 3507
Albuquerque, NM 87110
    ATTN J. Roger Hill

Science Applications, Inc.
8400 Westpark Drive
McLean, VA 22101
    ATTN William L. Chadsey

Singer Company (Data Systems), The
150 Totowa Road
Wayne, NJ 07470
    ATTN Tech Info Center

Singer Company, The
ATTN: Security Manager
1150 McBride Avenue
Little Falls, NJ 07424
    ATTN Irwin Goldman Eng Management

Sperry Flight Systems Division
Sperry Rand Corporation
P.O. Box 21111
Phoenix, AZ 85036
    ATTN D. Andrew Schow

Sperry Rand Corporation
Sperry Division
Marcus Avenue
Great Neck, NY 11020
    ATTN Charles L. Craig EV
    ATTN Paul Maraffino

Sperry Univac
Univac Park, P.O. Box 3525
St. Paul, MN 55165
    ATTN James A. Inda MS 41T25

SRI International
333 Ravenswood Avenue
Menlo Park, CA 94025
    ATTN Philip J. Dolan
    ATTN Arthur Lee Whitson

SRI International
306 Wynn Drive, NW
Huntsville, AL 35805
    ATTN MacPherson Morgan

Sundstrand Corporation
4751 Harrison Avenue
Rockford, IL 61101
    ATTN Curtis B. White

Systron-Donner Corporation
1090 San Miguel Road
Concord, CA 94518
    ATTN Gordon B. Dean
    ATTN Harold D. Morris

Texas Instruments, Inc.
P.O. Box 5474
Dallas, TX 75222
    ATTN Donald J. Manus MS 72

Texas Tech University
P.O. Box 5404 North College Station
Lubbock, TX 79417
    ATTN Travis L. Simpson

TRW Defense & Space Sys Group
One Space Park
Redondo Beach, CA 90278
    ATTN O. E. Adams R1-1144
    ATTN H. H. Holloway R1-2036
    ATTN Tech Info Center/S-1930
    ATTN R. K. Plebuch R1-2078
    ATTN Robert M. Webb R1-2410

TRW Defense & Space Sys Group
San Bernardino Operations
P.O. Box 1310
San Bernardino, CA 92402
    ATTN F. B. Fay
    ATTN R. Kitter

United Technologies Corporation
Hamilton Standard Division
Bradley International Airport
Windsor Locks, CT 06069
    ATTN Raymond G. Giguere

Vought Corporation
P.O. Box 5907
Dallas, TX 75222
    ATTN Technical Data Ctr

Westinghouse Electric Corporation
Defense and Electronic Systems Ctr
P.O. Box 1693
Baltimore-Washington Intl Airport
Baltimore, MD 21203
    ATTN Henry P. Kalapaca MS 3525

4. TITLE AND SUBTITLE Development of Hydrogen and Hydroxyl Contamination in Thin Silicon Dioxide Thermal Films		5. Publication Date March 1979
		6. Performing Organization Code

7. AUTHOR(S) Santos Mayo and William H. Evans	8. Performing Organ. Report No.

16. ABSTRACT (A 200-word or less factual summary of most significant information. If document includes a significant bibliography or literature survey, mention it here.)

Hydrogen and hydroxyl incorporation into thin silicon dioxide films thermally grown on silicon in dry oxygen atmospheres contained in resistance-heated fused silica or poly-crystalline silicon tubes is analyzed. The mechanisms leading to incorporation of these impurities in the film are discussed in terms of trace water and hydrocarbon contamination in the oxygen used, room ambient humidity permeation through the fused silica tube, the silicon wafer preparation prior to oxidation, and other environment factors. The most significant reactions occurring the water-silica-silicon system during wafer oxidation at temperatures in the range from 800°C to 1200°C are discussed. It is shown that, during the oxidation period required to grow a 100-nm thick silicon dioxide film on a <100> silicon wafer in nominally dry oxygen containing water contamination in the ppm range, the introduction of hydrogen and hydroxyl contamination into the oxide film can be explained in terms of the water-silica interaction. The use of polycrystalline silicon oxidation tubes is discussed with reference to the inherent water gettering action of silicon at oxidation temperatures.

17. KEY WORDS (six to twelve entries; alphabetical order; capitalize only the first letter of the first key word unless a proper name; separated by semicolons)

Dry oxidation of silicon; hydrogen contamination; hydroxyl contamination; semiconductor device fabrication; silicon; silicon dioxide; thermal oxidation of silicon.